 doi:10.20944/preprints202012.0383.v1

Discovery and Optimization of Selective Inhibitors of Meprin α (Part II)

Chao Wang[1], *Juan Diez*[2], *Hajeung Park*[1], *Christoph Becker-Pauly*[3], *Gregg B. Fields*[4], *Timothy P. Spicer*[1], *Louis D. Scampavia*[1], *Dmitriy Minond*[2,5], *and Thomas D. Bannister*[1]

[1] - Department of Molecular Medicine, Scripps Research, Jupiter, Florida 33458

[2] - Rumbaugh-Goodwin Institute for Cancer Research, Nova Southeastern University, 3321 College Avenue, CCR r.605, Fort Lauderdale, FL 33314

[3] - The Scripps Research Molecular Screening Center, Department of Molecular Medicine, Scripps Research, Jupiter, Florida 33458

[3] - University of Kiel, Institute of Biochemistry, Unit for Degradomics of the Protease Web, Rudolf-Höber-Str.1, 24118 Kiel, Germany

[4] - Department of Chemistry & Biochemistry and I-HEALTH, Florida Atlantic University, 5353 Parkside Drive, and Department of Chemistry, Scripps Research, Jupiter, FL 33458

[5]- Dr. Kiran C. Patel College of Allopathic Medicine, Nova Southeastern University, 3301 College Avenue, Fort Lauderdale, FL 33314

*Correspondence to: Thomas D. Bannister, 130 Scripps Way #A301, Jupiter, FL USA 33458; tbannist@scripps.edu

Short title: Chemical optimization of an inhibitor of meprin α

Subject category: medicinal chemistry

KEYWORDS: meprin α, meprin β, zinc metalloproteinase, medicinal chemistry, probe development

 doi:10.20944/preprints202012.0383.v1

ABSTRACT

Meprin α is a zinc metalloproteinase (metzincin) that has been implicated in multiple diseases, including fibrosis and cancers. It has proven difficult to find small molecules that are capable of selectively inhibiting meprin α, or its close relative meprin β, over numerous other metzincins which, if inhibited, would elicit unwanted effects. We recently identified possible molecular starting points for meprin α-specific inhibition through an HTS effort (see part I, preceding paper). In part II we report the optimization of a potent and selective hydroxamic acid meprin α inhibitor probe which may help define the therapeutic potential for small molecule meprin α inhibition and spur further drug discovery efforts in the area of zinc metalloproteinase inhibition.

INTRODUCTION

Meprin α is a zinc metalloproteinase (metzincin) that has been implicated in multiple diseases, including fibrosis[1,2], and cancers[3]. Understanding meprin α's precise role, alone or in combination with other metzincins, including its close relative meprin β, has been difficult to establish due to the lack of known selective inhibitors. While many preliminary reports for meprin inhibitors have emerged[4-8], no compounds with suitable potency, selectivity, and druglike attributes for *in vivo* use are known. We recently reported an HTS campaign to identify lead meprin α and meprin β inhibitors[9]. We then began SAR studies to understand the pharmacophore for meprin α inhibition, to enhance potency of the best leads, and to widen or maintain their selectivity over other metzincins. These efforts led to the identification of a probe molecule that may allow us in the future to ascertain the therapeutic potential for small molecule meprin α inhibition in the treatment of fibrosis or cancers.

 doi:10.20944/preprints202012.0383.v1

Zinc metalloproteinases are ubiquitous in human biology and their dysregulation in certain disease states has spurred many researchers to seek modulators, usually inhibitors, of their function. The primary difficulty in most drug discovery efforts is to gain selectivity for the zinc metalloproteinase of interest. Most inhibitors are characterized by "warhead" groups that bind zinc ions, often very tightly, if the warhead group is bidentate. Some of the more common zinc-binding warheads, either monodentate or bidentate, are shown in **Figure 1**. Using a warhead, especially bidentate, in an inhibitor gives an advantage in potency for the target, but also provides a disadvantage if the warhead is the main driver of potency. In such cases there is little opportunity for target selectivity over other zinc-containing enzymes. As a consequence, many such inhibitors block off-target zinc-containing enzymes that are required for a myriad of biological functions of healthy cells, resulting in intolerable toxicity. One common strategy is to avoid warhead groups altogether. A second strategy is to employ a warhead group that is: 1) consistent with drug-like properties, and 2) is attached to an organic molecule with several other functional groups that contribute substantially to its binding energy for the target, and not for other targets, thus imparting an acceptable level of target selectivity. Ideally this will translate to low toxicity in *in vivo* use. In our efforts here, our starting point was a hydroxamic acid-containing compound, as shown at the lower left in **Figure 1**.

Preprints (www.preprints.org) | NOT PEER-REVIEWED | Posted: 15 December 2020 doi:10.20944/preprints202012.0383.v1

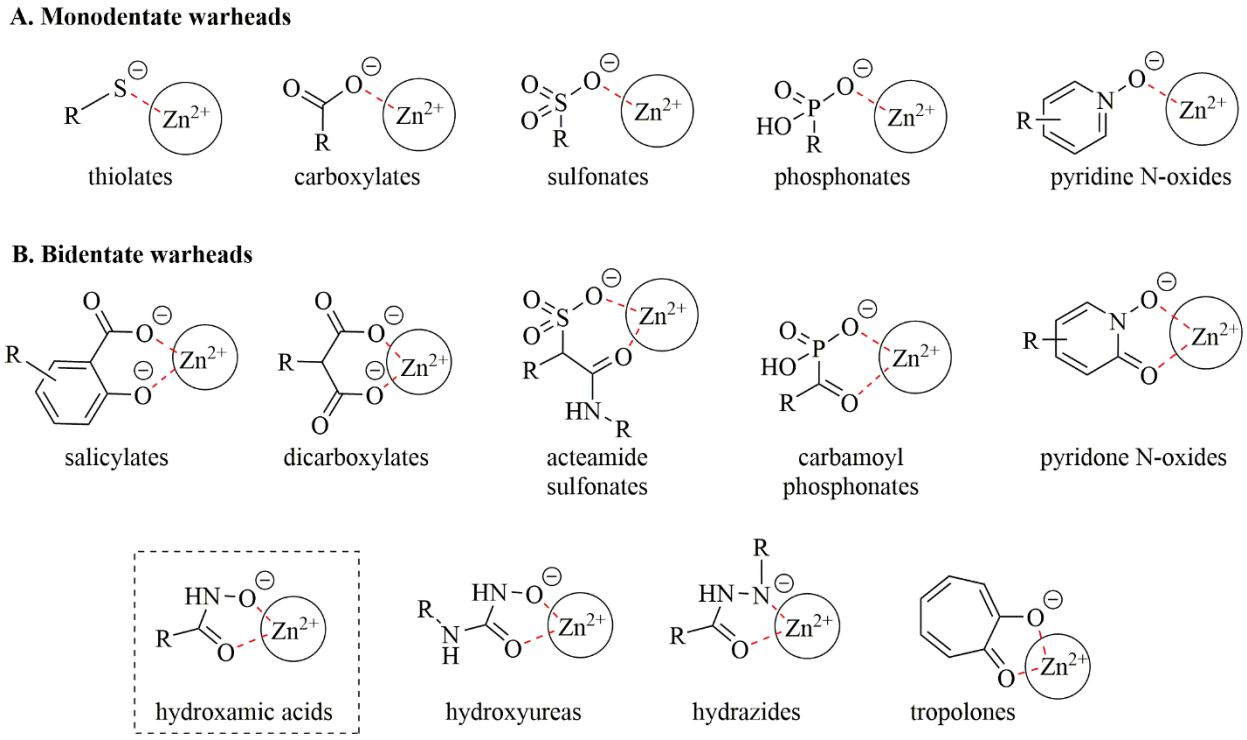

Figure 1. Zinc binding warheads

In our HTS effort we sought both warhead-containing and non-warhead-containing leads, but only warhead-containing leads were found to have suitable potency for follow-up. The presence of a warhead required that we address selectivity concerns at an early stage. The hydroxamic acid compound SR19855 (**Figure 2**) was found to be a low-micromolar inhibitor of meprin α with >20-fold selectivity over meprin β. It also has greater than 20-fold selectivity over a larger panel of metzincins: MMP-2, MMP-3, MMP-8, MMP-9, MMP-10, MMP-14, ADAM10, and ADAM17.

RESULTS

Modeling of lead series

Our HTS effort and follow-up SAR-by-purchase efforts identified a number of potent meprin α inhibitors bearing hydroxamic acid warheads. Among the most potent compounds were related aryl triazoles and thiadiazoles **(Figure 2**). Notably, the thiadiazoles were unlike the aryl triazoles in terms of isoform selectivity: only the aryl triazoles were selective for meprin α over meprin β.

Preprints (www.preprints.org) | NOT PEER-REVIEWED | Posted: 15 December 2020 doi:10.20944/preprints202012.0383.v1

We surmised that the additional aromatic ring in the aryl triazoles may be an important selectivity element favoring binding to meprin α over meprin β, and perhaps over other metzincins as well. A purchased analog in the series showed a preference for a *para*-methoxy group in the central aromatic ring. In the thiadiazole series, similar compounds purchased with a thiazole core (one N replaced with CH) were less potent, suggesting that the nitrogen atoms in the central heterocycle were of some importance.

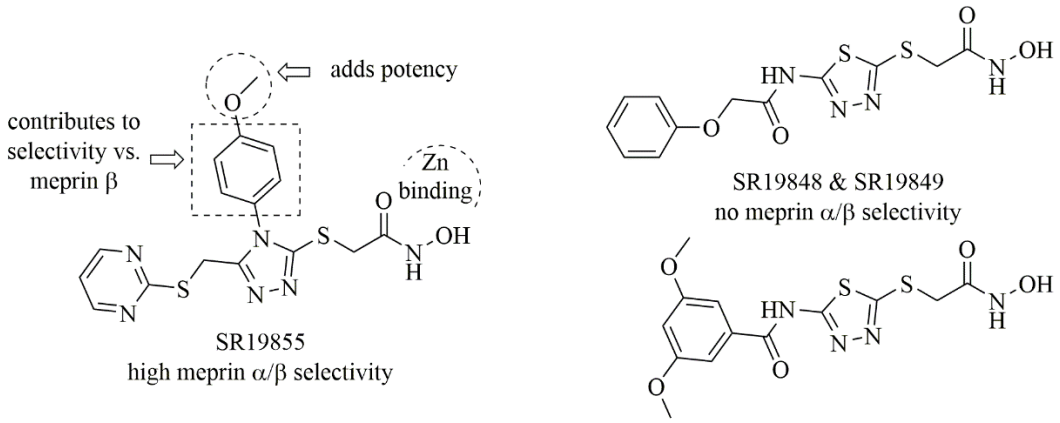

Figure 2. HTS hit SR19855 and related thiadiazoles

We wished to understand the possible basis for meprin α binding and selectivity. The crystal structure of human meprin β (PDB ID 4GWN) was used as a template for constructing a model of human meprin α using Prime (Schrodinger, LLC, NY), with the option of a single template to build a single chain and including the Zn ion. The homology model and the coordinates, 4GWN, were prepared using the protein preparation wizard in Maestro v12.2 (Schrodinger, LLC, NY). Docking studies were performed using Glide SP v8.7 (Schrodinger, LLC, NY) with no constraint. The docking grid was generated around the Zn ion with a box size of 18 X 18 X 18 Å3. SR19855 was prepared for Glide docking with LigPrep (Schrodinger, LLC, NY) to include different conformational states. The docking pose with the highest docking score for each compound was

 doi:10.20944/preprints202012.0383.v1

then merged to the docked structures for energy minimization using the OPLS3e force field (Schrodinger, LLC, NY) and the results were analyzed in pymol.

A strong bidentate interaction, as expected, is seen between the hydroxamate of SR19885 and the Zn ion in both docking models (**Figure 3**). This binding anchors the ligand into each active site. Overall, geometry of binding for the backbone of the ligand is similar. Important differences are apparent for the side chains, however, especially the interactions of the central *para*-methoxy phenyl group in meprin α. As shown in the left panel of **Figure 3**, Y214 of meprin α makes a face-on π-π interaction with the phenyl ring. R242 makes cation-π interactions with both phenyl and pyrimidine rings of the ligand. Although the primary sequences of the meprin isoforms are similar in the binding pocket, these interactions are absent or are much weaker in meprin β with the exception of the warhead/Zn interaction and an H-bond interaction to Y211 (Y214 in meprin α) that are preserved. These findings suggest that the aryl triazole core of the ligand be preserved, for selectivity purposes, during our SAR studies aimed to increase potency and selectivity for meprin α.

Preprints (www.preprints.org) | NOT PEER-REVIEWED | Posted: 15 December 2020 doi:10.20944/preprints202012.0383.v1

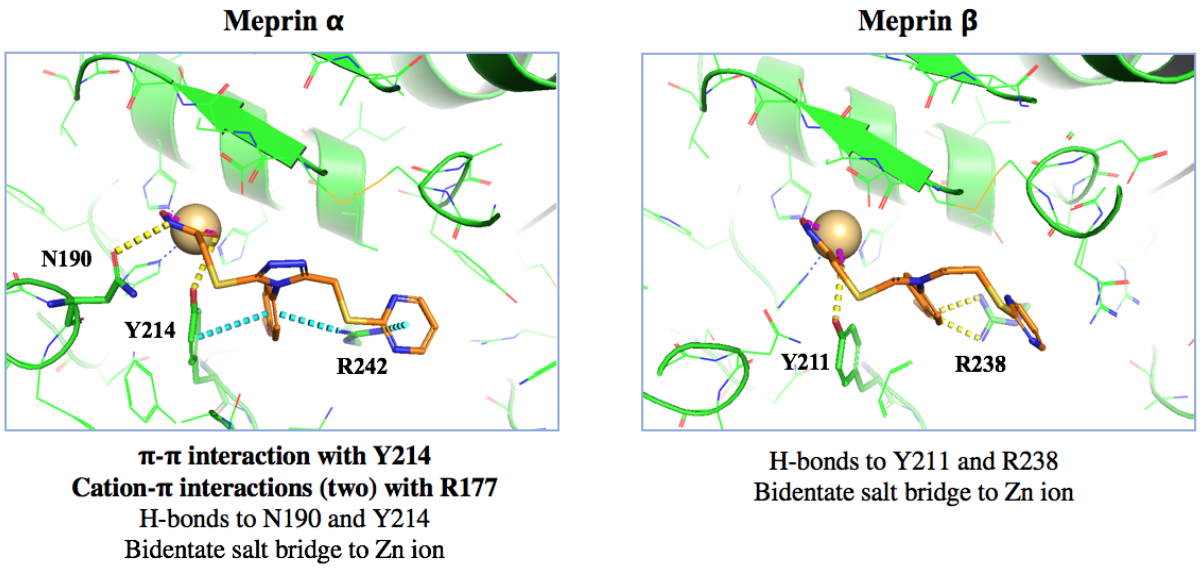

Figure 3. SR19855 docked to meprins α and β

Guided by structure activity relationships seen in the HTS effort and purchased analogs, we wished to broadly explore structural variations to maximize potency and to maintain target selectivity, looking especially at substituent effects in the pyrimidine and phenyl rings (as shown in **Figure 4**).

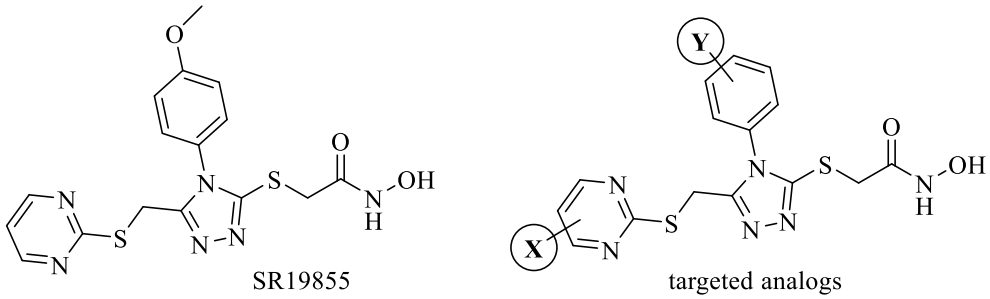

Figure 4. HTS hit SR19855 and targeted analogs

Synthetic strategy

To further study compounds in the series we initiated an internal synthesis effort. A versatile 5-step synthesis used is shown in **Figure 5**, which is adaptable for different X and Y groups on the pyrimidine and phenyl rings, respectively. This strategy is based upon the initial 3 steps of a

Preprints (www.preprints.org) | NOT PEER-REVIEWED | Posted: 15 December 2020 doi:10.20944/preprints202012.0383.v1

literature method[10]. Briefly, the alkylation of a thiopyrimidine is followed by treatment with hydrazine to form a hydrazine amide, which is acylated with an isothiocyanate. Acidic workup gives the mercaptotriazole, which is then alkylated with an alkyl chloride. Finally, the warhead is installed by treatment with hydroxylamine.

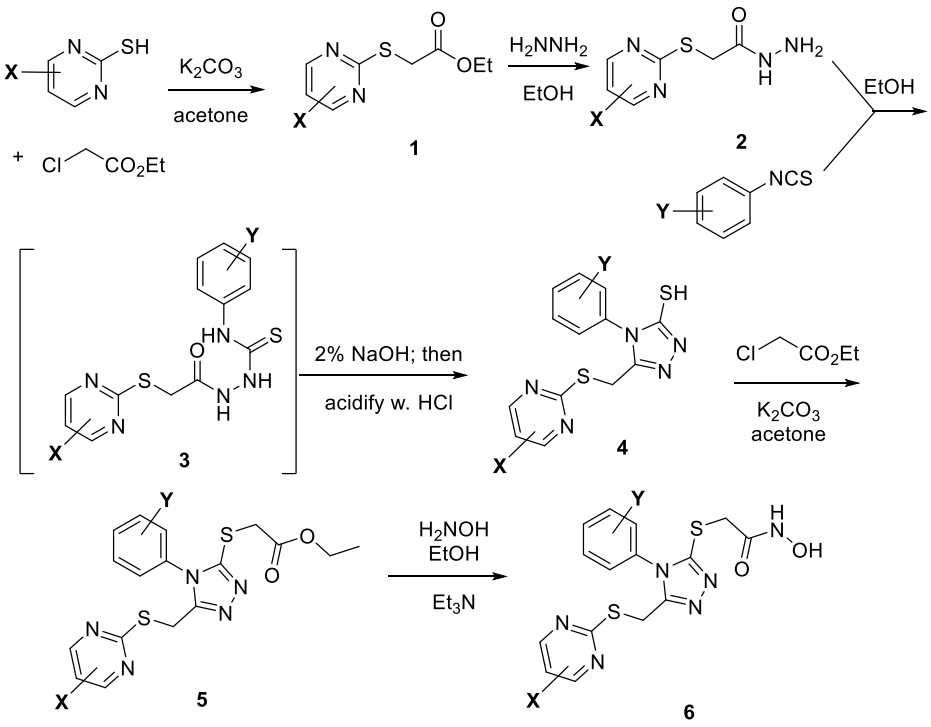

Figure 5. General synthesis scheme

1. Pyrimidine substitution

We investigated varying the X group(s), making monosubstituted and disubstituted pyrimidines (**Figure 6**), with Y held constant as *para*-methoxy. An electron deficient pyrimidine (3-CF_3) was a less potent meprin α binder (IC_{50} = 14 μM) than was the unsubstituted pyrimidine HTS hit SR19855 (IC_{50} = 1.3 μM) though it was selective vs. meprin β (IC_{50} > 100 μM). A neutral pyrimidine (3,5-dimethyl) was an intermediate meprin α binder (IC_{50} = 4.1 μM) but showed some meprin β affinity as well ((IC_{50} = 600 μM). An electron deficient pyrimidine (3,5-dimethoxy)

Preprints (www.preprints.org) | NOT PEER-REVIEWED | Posted: 15 December 2020 doi:10.20944/preprints202012.0383.v1

maximized selectivity, which was our primary criteria for probe development, provided that affinity could also be increased in subsequent analogs (meprin α IC_{50} = 8.7 μM, meprin β IC_{50} >>100 μM). The absence of inhibition of meprin β at 100 μM led us to use the 3,5-dimethoxypyrimidine in a round of analogs aimed at optimizing the Y group.

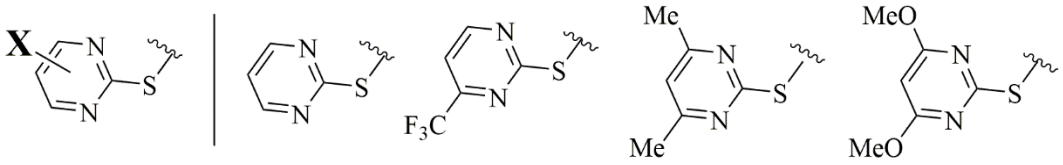

Figure 6. Pyrimidines investigated

2. Phenyl substitution

Substitution in the phenyl ring by group Y (**Figure 7**) had a more dramatic effect on meprin α binding affinity. Adding a *para* or *meta* chloro group greatly reduced activity (meprin α IC_{50} >100 μM, 30 μM, respectively). Other electron-withdrawing or neutral *para* or *meta* groups (NO_2, Br, CF_3, Me) gave modest meprin α binding, with IC_{50} values in the range of 5-10 μM. The electron rich 3,4-methylenedioxy analog was modestly more potent (IC_{50} = 4.2 μM). We saw the greatest boost in potency when a *para* amino substituent Y was added, with the 4-morpholine analog having an IC_{50} = 1.1 μM and the 4-dimethylamino analog having an IC_{50} = 600 nM. This IC_{50} was consistent over 4 replicates, ranging from 490-670 nM. Selectivity over meprin β was maintained in all analogs (IC_{50} >100 μM). To test our presumption that the hydroxamic acid is essential, we also tested certain ester synthetic precursors to the hydroxamates and saw no activity (meprin α IC_{50} > 100 μM).

Preprints (www.preprints.org) | NOT PEER-REVIEWED | Posted: 15 December 2020 doi:10.20944/preprints202012.0383.v1

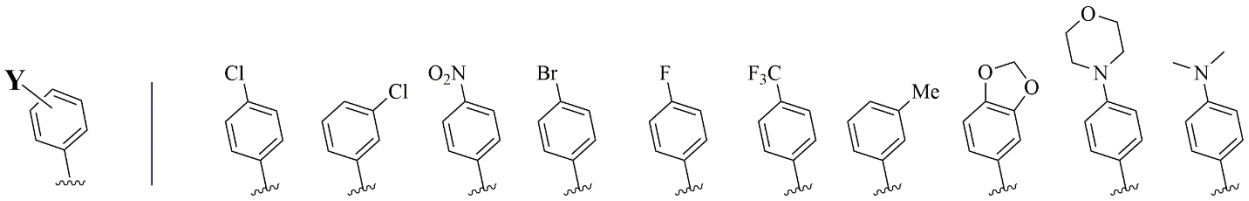

Figure 7. Central phenyl substitutions investigated

3. Probe synthesis: SR24717

Following the general synthesis scheme from **Figure 5**, the probe molecule, combining high potency with high selectivity, was prepared in 5 steps (**Figure 8**). Synthetic methods and characterization are described in the Materials and Methods section.

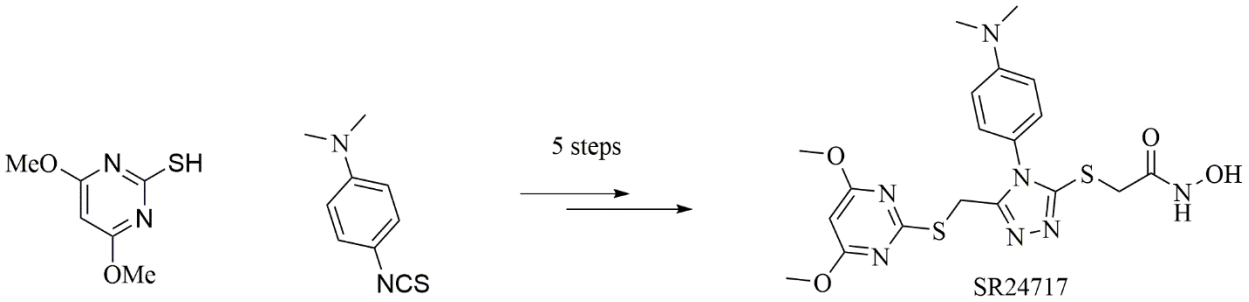

Figure 8. SR24717 (meprin α probe) synthesis

Probe characterization in *in vitro* assays

We tested a freshly re-synthesized, analytically pure sample of SR24717 against meprin α, meprin β, and related metzincins. IC_{50} values for SR24717 were batch independent (IC_{50} meprin α = 662 nM and 490-670 nM, respectively; IC_{50} meprin β = 70 µM and 100 µM, respectively) (**Figure 9A**). Assay results with related metzincins demonstrated excellent broad selectivity of SR24717 (IC_{50} metzincins > 100 µM for all tested enzymes, **Figure 9B**).

Preprints (www.preprints.org) | NOT PEER-REVIEWED | Posted: 15 December 2020 doi:10.20944/preprints202012.0383.v1

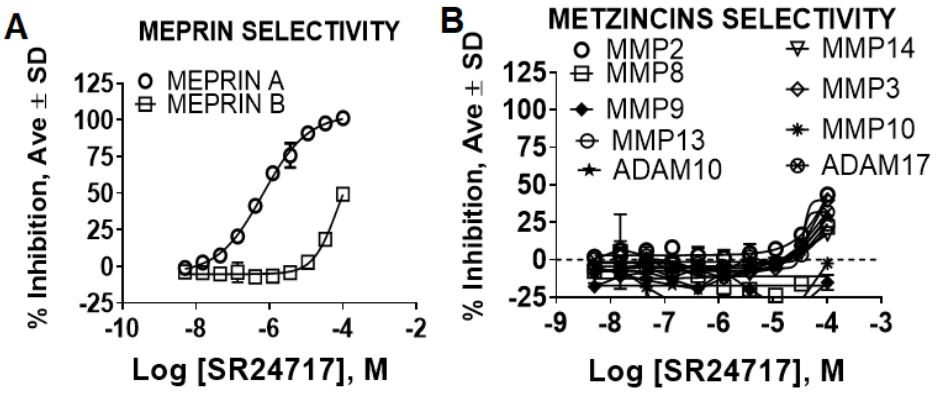

Figure 9. Characterization of meprin α probe SR24717 against meprin β and related metzincins. (A) Dose response study of re-synthesis batch of SR24717 with meprin α and β shows reproducibility with the original batch; (B) Dose response study of re-synthesis of SR24717 with metzincins shows good selectivity profile. All experiments performed as 10 point 3-fold concentration-response curves in triplicate. All units are IC_{50}, µM.

We further characterized SR24717 for the mode of inhibition of meprin α. Pre-incubation of SR24717 with meprin α for 0-3 h showed no change in IC_{50} values, suggesting that SR24717 is not a time dependent inhibitor (**Figure 10A**). This allowed us to use steady-state assumption in our follow up experiments. Varying substrate concentration in meprin α decreased the apparent potency of SR24717 (**Figures 10B and C**), suggesting a competitive mode of inhibition. Indeed, both linear (**Figure 10D**) and non-linear (**Figure 10E**) models showed good fit to the competitive inhibition. Global fit to the competitive model of inhibition using GraphPad Prizm showed K_i = 300.8 nM.

We tested SR24717 for effects on viability and cytotoxicity of several cell types. Only at a concentration of 100 µM of SR24717 were negative effects on viability and cytotoxicity observed (**Figure 11**) suggesting that SR24717 can be a useful probe for studying the biological role of meprin α in *in vitro* and *in vivo* systems.

Preprints (www.preprints.org) | NOT PEER-REVIEWED | Posted: 15 December 2020 doi:10.20944/preprints202012.0383.v1

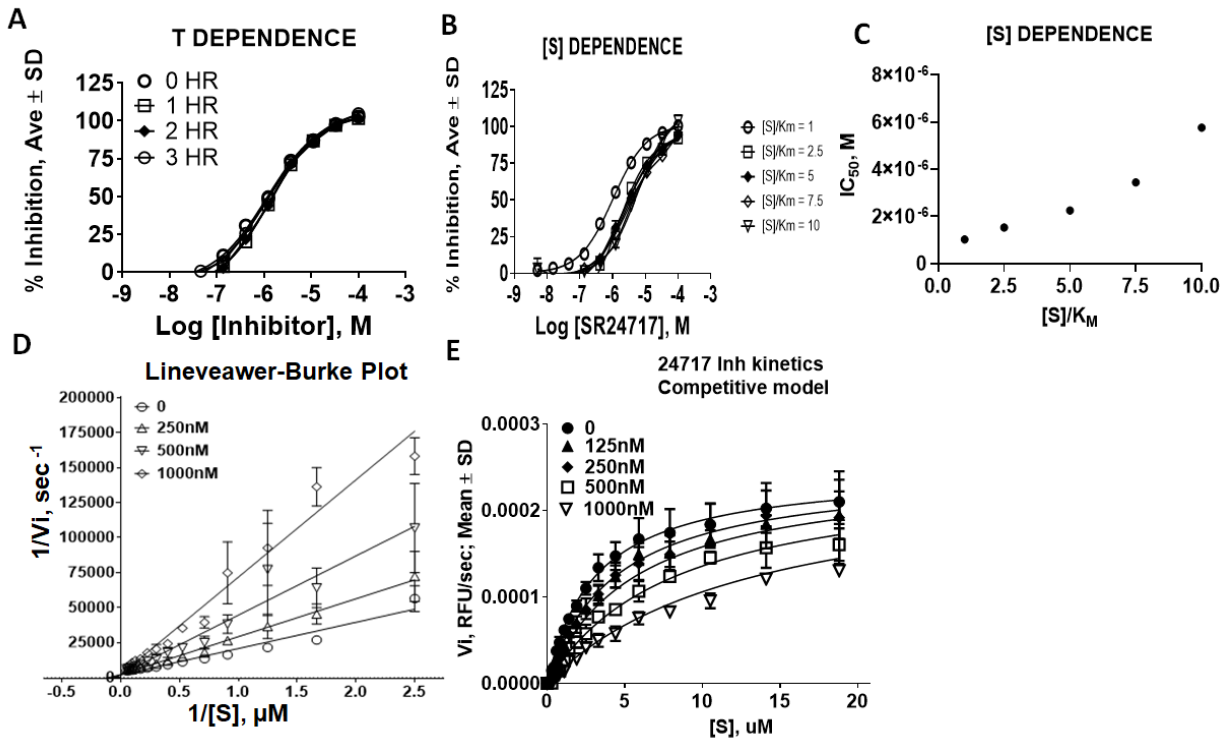

Figure 10. Characterization of meprin α probe candidate SR24717 mode of enzyme inhibition. (A) Time dependence study of inhibition of meprin α mediated proteolysis by SR24717; (B) Substrate concentration dependence study of inhibition of meprin α mediated proteolysis by SR24717; (C) Re-plot of (B) shows increase of IC_{50} values correlating with increase of substrate concentration suggestive of competitive inhibition mechanism by SR24717; (D) Lineweaver-Burke plot shows lines of best fit crossing at Y-axis suggesting a competitive inhibition mechanism by SR24717; (E) Global fit of meprin α mediated proteolysis in the presence of SR24717 to competitive model using non-linear regression shows good fit.

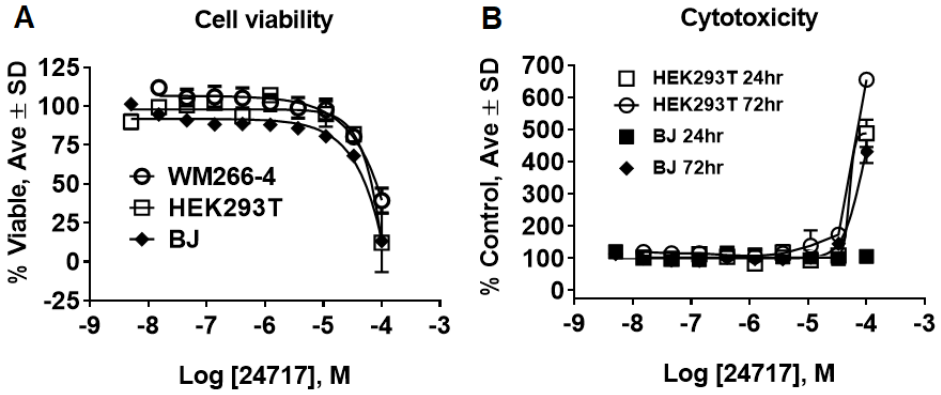

Figure 11. Characterization of meprin α probe candidate SR24717 for effect on cell viability and cytotoxicity. (A) Effect of SR24717 on viability of WM266-4 (skin melanoma), HEK293 (kidney), and BJ (skin fibroblasts) cells. CellTiter Glo™ assay (Promega) was used after 72h treatment; (B) Effect of SR24717 on viability of HEK293 (kidney), and BJ (skin fibroblasts) cells. CellTox Green™ assay (Promega) was used. All experiments performed as 10 point 3-fold concentration-response curves in triplicate.

Preprints (www.preprints.org) | NOT PEER-REVIEWED | Posted: 15 December 2020 doi:10.20944/preprints202012.0383.v1

DISCUSSSION

The modeling study described earlier had suggested the importance of cation-π interactions for meprin α potency and selectivity. Our structure-activity relationship study supports the model, in that the 3,5-dimethoxypyrimidine and 4-dimethylaminophenyl groups of the probe molecule SR24717 work in concert to augment potency and selectivity. Though SR24717 is merely ~2-fold more potent than the HTS hit SR19855 in binding meprin α, it has selectivity advantages, with generally lower IC_{50} and/or lower maximum inhibition of other metzincins tested even at the highest concentration studied (100 μM). Future work toward optimization of a meprin α probe includes the evaluation and optimization of DMPK properties for *in vivo* use, while maintaining target potency and selectivity.

Table 1. Affinity and selectivity of SR24717 vs SR19855 and literature reference compounds 10d and 10e.[11]

ID	**Meprin α** IC_{50}, μM	**Meprin β** IC_{50}, μM	**Selectivity Fold**
SR24717 (probe)	0.66	>70	>100
SR19855 (HTS hit)	1.3	>17.0	>13
10d (ref 11)	0.16	2.95	18
10e (ref 11)	0.40	7.59	19

MATERIALS AND METHODS

Assay Reagents. MMP-1, MMP-2, MMP-8, MMP-9, MMP-10, MMP-13, MMP-14, ADAM10, ADAM17 and Mca-KPLGL-Dpa-AR-NH_2 fluorogenic peptide substrate were purchased from R&D Systems (cat # 901-MP, 902-MP, 908-MP, 911-MP, 910-MP, 511-MM, 918-MP, 936-AD, 930-ADB, and ES010, respectively). All common chemicals were purchased from Sigma. NFF449 was purchased from Tocris (cat# 1391) and actinonin was from Sigma-Aldrich (cat# 01809).

Preprints (www.preprints.org) | NOT PEER-REVIEWED | Posted: 15 December 2020 doi:10.20944/preprints202012.0383.v1

Meprin α and meprin β substrate synthesis. Meprin α and meprin β substrates (Mca-YVADAPK-(K-ε-Dnp) and Mca-EDEDED-(K-ε-Dnp), respectively)[12] were synthesized according to Fmoc solid-phase methodology on a peptide synthesizer. All peptides were synthesized as C-terminal amides to prevent diketopiperazine formation[13]. Cleavage and side-chain deprotection of peptide-resins was for at least 2 h using thioanisole-water-TFA (5:5:90). The substrates were purified and characterized by preparative RP HPLC and characterized by MALDI-TOF MS and analytical RP HPLC.

Meprins expression protocol. Recombinant human meprin α and meprin β were expressed using the Bac-to-Bac expression system (Gibco Life Technologies, Paisley, UK) as described before[14,15]. Media and supplements were obtained from Gibco Life Technologies. Recombinant Baculoviruses were amplified in adherently growing *Spodoptera frugiperda* (*Sf*)9 insect cells at 27°C in Grace's insect medium supplemented with 10% fetal bovine serum, 50 units/mL penicillin and 50 µg/mL streptomycin. Protein expression was performed in 500 mL suspension cultures of BTI-TN-5B1-4 insect cells growing in Express Five SFM supplemented with 4 mM glutamine, 50 units/mL penicillin and 50 µg/mL streptomycin in Fernbach-flasks using a Multitron orbital shaker (INFORS AG, Bottmingen, Switzerland). Cells were infected at a density of 2×10^6 cells/mL with an amplified viral stock at a MOI of ~10. Protein expression was stopped after 72 h, and recombinant meprins were further purified from the media by ammonium sulfate precipitation (60% saturation) and affinity chromatography (Strep-tactin for Strep-tagged meprin α and Ni-NTA for His-tagged meprin β). Meprins were activated by trypsin, which was removed afterwards by affinity chromatography using a column containing immobilized chicken ovomucoid, a trypsin inhibitor.

Preprints (www.preprints.org) | NOT PEER-REVIEWED | Posted: 15 December 2020 doi:10.20944/preprints202012.0383.v1

Meprin α and meprin β assays in 384 well plate. Both assays followed the same general protocol[16]. 5 µL of 2x enzyme solution (2.6 and 0.1 nM for meprin α and meprin β, respectively) in assay buffer (50 mM HEPES, 0.01% Brij-35, pH 7.5) were added to solid bottom black 384 low volume plates (Nunc, cat# 264705). Next, 75 nL of test compounds or pharmacological control (actinonin) were added to corresponding wells using a 384-pin tool device (V&P Scientific, San Diego). After 30 min incubation at RT, the reactions were started by addition of 5 µL of 2x solutions of substrates (20 µM, meprin α Mca-YVADAPK-K(Dnp); and for meprin β Mca-EDEDED-K(Dnp)). Reactions were incubated at RT for 1 h, after which the fluorescence was measured using the Synergy H4 multimode microplate reader (Biotek Instruments) ($\lambda_{excitation}$ = 324 nm, $\lambda_{emission}$ = 390 nm).

Three parameters were calculated on a per-plate basis: (a) the signal-to-background ratio (S/B); (b) the coefficient for variation [CV; CV = (standard deviation/mean) x 100)] for all compound test wells; and (c) the Z- or Z'-factor [7]. Z takes into account the effect of test compounds on the assay window, while Z' is based on controls.

Determination of kinetic parameters of meprin α mediated proteolysis in the presence of probe SR24717. Substrate stock solutions were prepared at various concentrations in HTS assay buffer (50 mM HEPES, 0.01% Brij-35, pH 7.5). Assays were conducted by incubating a range of substrate (2-50 µM) and SR24717 concentrations (0-1000 nM) with 1.3 nM meprinα at 25 °C. Fluorescence was measured on a multimode microplate reader Synergy H1 (Biotek Instruments, Winooski, VT) using $\lambda_{excitation}$ = 324 nm and $\lambda_{emission}$ = 393 nm. Rates of hydrolysis were obtained from plots of fluorescence versus time, using data points from only the linear portion of the hydrolysis curve. The slope from these plots was divided by the fluorescence change corresponding to complete hydrolysis and then multiplied by the substrate concentration to obtain

Preprints (www.preprints.org) | NOT PEER-REVIEWED | Posted: 15 December 2020 doi:10.20944/preprints202012.0383.v1

rates of hydrolysis in units of μM/s. Kinetic parameters were calculated by non-linear regression analysis using the GraphPad Prism 8.0 suite of programs.

ADAM10 and ADAM17 assays. Both assays followed the same general protocol. 2.5 μL of 2x enzyme solution (20 nM) in assay buffer (10 mM HEPES, 0.001% Brij-35, pH 7.5) were added to solid bottom black 384 plates (Greiner, cat# 789075). Next, test compounds and pharmacological controls were added to corresponding wells using a 384 pin tool device (V&P Scientific, San Diego). After 30 min incubation at RT, the reactions were started by addition of 2.5 μL of 2x solutions of substrate (R&D Systems cat#: ES010, Mca-KPLGL-Dpa-AR-NH_2, 20 μM). Reactions were incubated at RT for 2 h, after which the fluorescence was measured using Perkin Elmer Viewlux multimode microplate imager ($\lambda_{excitation}$ = 324 nm, $\lambda_{emission}$ = 393 nm). All compounds were tested in 10-point, 1:3 serial dilutions dose-response format starting with highest concentration of 100 μM. IC_{50} values were determined using non-linear regression analysis using the GraphPad Prism 8.0 suite of programs.

MMP assays. All assays followed the same general protocol. 5 μL of 2x enzyme solution (5 nM) in assay buffer (50 mM Tricine, 50mM NaCl, 10mM $CaCl_2$, 0.05% Brij-35, pH 7.5) were added to solid bottom black 384 plates (Nunc, cat# 264705). Next, test compounds and pharmacological controls were added to corresponding wells using a 384-pin tool device (V&P Scientific, San Diego). After 30 min incubation at RT, the reactions were started by addition of 5 μL of 2x solutions of MMP substrate (R&D Systems cat#: ES010, 20 μM). Reactions were incubated at RT for 1 h, after which the fluorescence was measured using the Synergy H4 multimode microplate reader (Biotek Instruments) ($\lambda_{excitation}$ = 324 nm, $\lambda_{emission}$ = 390 nm). All compounds were tested in 10-point, 1:3 serial dilutions dose-response format starting with highest concentration of 100 μM.

Preprints (www.preprints.org) | NOT PEER-REVIEWED | Posted: 15 December 2020 doi:10.20944/preprints202012.0383.v1

IC_{50} values were determined using non-linear regression analysis using the GraphPad Prism 8.0 suite of programs.

Cell toxicity studies. Test compounds were solubilized in 100% DMSO and added to polypropylene 384 well plates (Greiner cat# 781280). 1,250 of BJ skin fibroblasts or primary melanocytes were plated in 384-well plates in 8 µL of serum-free media (HybriCare for BT474, EMEM for HEK293). Test compounds and pharmacological assay control (lapatinib) were prepared as 10-point, 1:3 serial dilutions starting at 10 mM, then added to the cells using the pin tool mounted on Integra 384. Plates were incubated for 72 h at 37 °C, 5% CO_2 and 95% RH. After incubation, 8 µL of CellTiter-Glo® (Promega cat# G7570) was added to each well and incubated for 15 min at room temperature. Luminescence was recorded using a Biotek Synergy H1 multimode microplate reader. Viability was expressed as a percentage relative to wells containing media only (0%) and wells containing cells treated with DMSO only (100%). Three parameters were calculated on a per-plate basis: (a) the signal-to-background ratio (S/B); (b) the coefficient for variation [CV; CV = (standard deviation/mean) x 100)] for all compound test wells; and (c) the Z'-factor. IC_{50} values were calculated by fitting normalized data to sigmoidal log vs. response equation utilizing non-linear regression analysis from GraphPad Prizm 8.

Probe SR24717 synthesis and characterization. Synthesis of all test compounds followed the 5-step route summarized in **Figure 5** with steps 1-3 adapted from the literature.[18,19]

Step 1, Ethyl 2-[(aryl)thio] acetate derivatives (**1**). Mercaptopyrimidine (1 equiv.), ethyl 2-chloroacetate (2 equiv.) and potassium carbonate (1.2 equiv.) were heated at 80 °C in acetone. Reaction progress was monitored by LC/MS and after 2 hours the mixture was cooled, filtered, and concentrated to give the crude product in >75% yield as a solid (>95% purity by LC/MS), used in the next step without further purification.

Preprints (www.preprints.org) | NOT PEER-REVIEWED | Posted: 15 December 2020 doi:10.20944/preprints202012.0383.v1

.

Step 2, 2-[(Aryl)thio]acetohydrazide derivatives (**2**). A mixture of ethyl 2-[(aryl)thio]acetate (**1**) (1 equiv.) and hydrazine hydrate (2 equiv.) in ethanol was stirred for 1-2 hours at room temperature, then the colorless solid (>95% purity by LC/MS), was filtered, washed with water, dried, and taken to the next step without purification.

Step 3. Thiosemicarbazide derivatives (**3**). A mixture of the hydrazide (**2**) (1 equiv.) and a phenyl isothiocyanate (1 equiv.) in ethanol was refluxed for 1 h. The mixture was cooled, filtered, concentrated, and the product (>95% pure by LC/MS) was taken to the next step without purification.

Step 4, Mercaptotriazole derivatives (**4**). A suspension of thiosemicarbazide (**3**) in aq. 2% NaOH was heated at 100 °C for 30 min-2 h then cooled to room temperature. The pH was adjusted to 6-7 by the addition of 3M HCl. The mixture filtered and dried to give a colorless solid as product (>95% pure by LC/MS, 70% isolated yield for steps 2-4).

Step 5, Mercaptotriazole esters (**5**). A mixture of the mercaptotriazole (**4**) (1 equiv.), ethyl 2-chloroacetate (1.12 equiv.) and potassium carbonate (1.5 equiv.) in acetone was heated at 80 °C for 0.5-2 h. The reaction was monitored by LC/MS. After completion, the reaction mixture was cooled, filtered to give the crude product as a pale-yellow solid in near quantitative yield and >95% purity. This solid was then used in the next step without further purification.

Step 6, final hydroxamic acids (**6**). A solution of mercaptotriazole ester (**5**) (1 equiv.) in MeOH/DCM (3:1) cooled to 0 °C was treated with saturated hydroxylamine hydrochloride solution (6 equiv.) followed by the addition of sat. aq. NaOH (12 equiv.). After reaction completion (typically~10 min) the mixture was concentrated *in vacuo*, water was added, the pH was adjusted

 doi:10.20944/preprints202012.0383.v1

to 7 by the addition of 2M HCl. The colorless solid product (25-30% yield, >95% analytical purity) was collected by filtration.[20] Characterization data for the probe SR24717: **^{1}H NMR** (600 MHz, DMSO-d6): δ ppm 10.75 (s, 1H), 9.01 (s, 1H), 8.58 (s, 1H), 7.16 (d, *J* = 8.8 Hz, 2H), 6.68 (d, *J* = 8.8 Hz, 2H), 5.89 (s, 1H), 6.94 (s, 1H), 4.48 (s, 2H), 3.81 (s, 6H), 3.78 (s, 2H), 2.94 (s, 6H). **^{13}C NMR** (DMSO-d6): δ ppm 170.9,168.2, 164.2, 153.7, 151.9, 151.2, 128.4, 120.3, 112.4, 86.0, 60.2, 33.4, 24.4. MS (ESI, M + H) calculated for ($C_{19}H_{23}N_7O_4S_2$ + H): 478.13, found 477.86, purity by analytical HPLC > 92%.

AUTHOR INFORMATION

Corresponding author

*Email: tbannist@scripps.edu

Abbreviations

MMP - matrix metalloprotease; ADAM - a disintegrin and metalloprotease.

Acknowledgements and funding sources

This work was supported by the National Institutes of Health (AR066676 and CA249788 to DM). This work was also supported by the Deutsche Forschungsgemeinschaft (DFG) grant SFB877 “Proteolysis as a Regulatory Event in Pathophysiology” (project A9 and A15) (both to C.B.-P.). We thank Pierre Baillargeon and Lina DeLuca (Lead Identification, Scripps Florida) for compound management.

Author contributions statement

C.W. and T.B. designed the compounds, C.W. performed all compound synthesis and characterization, H.P. performed modeling studies, J.D. performed cytotoxicity studies, G.B.F

synthesized, purified, and characterized meprin α and meprin β substrates, C.B.P. expressed meprin α and meprin β, L.D.S. and T.P.S. provided compound management support, D.M. provided program oversight, designed the assays, performed post-HTS biochemical *in vitro* characterization of hits, and T.B. wrote the main manuscript text and prepared figures, while all other authors provided edits, additions, and review.

Notes

The authors declare no competing financial interests.

REFERENCES

1. Prox, J.; Arnold, P.; Becker-Pauly, C., Meprin alpha and meprin beta: Procollagen proteinases in health and disease. *Matrix Biol* **2015,** *44-46*, 7-13.
2. Broder, C.; Arnold, P.; Vadon-Le Goff, S.; Konerding, M. A.; Bahr, K.; Muller, S.; Overall, C. M.; Bond, J. S.; Koudelka, T.; Tholey, A.; Hulmes, D. J.; Moali, C.; Becker-Pauly, C., Metalloproteases meprin alpha and meprin beta are C- and N-procollagen proteinases important for collagen assembly and tensile strength. *Proc Natl Acad Sci U S A* **2013,** *110* (35), 14219-24.
3. Peters, F.; Becker-Pauly, C., Role of meprin metalloproteases in metastasis and tumor microenvironment. *Cancer Metastasis Rev* **2019,** *38* (3), 347-356
4. Kruse, M. N.; Becker, C.; Lottaz, D.; Kohler, D.; Yiallouros, I.; Krell, H. W.; Sterchi, E. E.; Stocker, W., Human meprin alpha and beta homo-oligomers: cleavage of basement membrane proteins and sensitivity to metalloprotease inhibitors. *Biochem J* **2004,** *378* (Pt 2), 383-9.
5. Madoux, F.; Tredup, C.; Spicer, T. P.; Scampavia, L.; Chase, P. S.; Hodder, P. S.; Fields, G. B.; Becker-Pauly, C.; Minond, D., Development of high throughput screening assays and pilot screen for inhibitors of metalloproteases meprin alpha and beta. *Biopolymers* **2014,** *102* (5), 396-406.
6. Ramsbeck, D.; Hamann, A.; Schlenzig, D.; Schilling, S.; Buchholz, M., First insight into structure-activity relationships of selective meprin beta inhibitors. *Bioorg Med Chem Lett* **2017,** *27* (11), 2428-2431.
7. Ramsbeck, D.; Hamann, A.; Richter, G.; Schlenzig, D.; Geissler, S.; Nykiel, V.; Cynis, H.; Schilling, S.; Buchholz, M., Structure-Guided Design, Synthesis, and Characterization of Next-Generation Meprin beta Inhibitors. *J Med Chem* **2018,** *61* (10), 4578-4592.
8. Tan, K.; Jager, C.; Schlenzig, D.; Schilling, S.; Buchholz, M.; Ramsbeck, D., Tertiary-Amine-Based Inhibitors of the Astacin Protease Meprin alpha. *ChemMedChem* **2018,** *13* (16), 1619-1624.
9. See preceeding paper in this issue.
10. Altintop, M. D.; Kaplancikli, Z. A.; Ciftci, G. A.; Demirel, R. Synthesis and biological evaluation of thiazoline derivatives as newantimicrobial and anticancer agents. *Eur. J. Med. Chem*. 2014, 74, 264-277.

11. Tan, K.; Jager, C.; Schlenzig, D.; Schilling, S.; Buchholz, M.; Ramsbeck, D., Tertiary-Amine-Based Inhibitors of the Astacin Protease Meprin alpha. *ChemMedChem* **2018,** *13* (16), 1619-1624.
12. Broder, C.; Becker-Pauly, C., The metalloproteases meprin alpha and meprin beta: unique enzymes in inflammation, neurodegeneration, cancer and fibrosis. *Biochem J* **2013,** *450* (2), 253-64.
13. Fields, G. B.; Lauer-Fields, J. L.; Liu, R.-q.; Barany, G., Principles and Practice of Solid-Phase Peptide Synthesis. In *Synthetic Peptides: A User's Guide*, 2nd ed.; Grant, G. A., Ed. W.H. Freeman & Co.: New York, 2001; pp 93-219.
14. de Jong, G. I.; Buwalda, B.; Schuurman, T.; Luiten, P. G., Synaptic plasticity in the dentate gyrus of aged rats is altered after chronic nimodipine application. *Brain Res* **1992,** *596* (1-2), 345-8.
15. Becker-Pauly, C.; Howel, M.; Walker, T.; Vlad, A.; Aufenvenne, K.; Oji, V.; Lottaz, D.; Sterchi, E. E.; Debela, M.; Magdolen, V.; Traupe, H.; Stocker, W., The alpha and beta subunits of the metalloprotease meprin are expressed in separate layers of human epidermis, revealing different functions in keratinocyte proliferation and differentiation. *J Invest Dermatol* **2007,** *127* (5), 1115-25.
16. Madoux, F.; Tredup, C.; Spicer, T. P.; Scampavia, L.; Chase, P. S.; Hodder, P. S.; Fields, G. B.; Becker-Pauly, C.; Minond, D., Development of high throughput screening assays and pilot screen for inhibitors of metalloproteases meprin alpha and beta. *Biopolymers* **2014,** *102* (5), 396-406.
17. Zhang, J. H.; Chung, T. D.; Oldenburg, K. R., A Simple Statistical Parameter for Use in Evaluation and Validation of High Throughput Screening Assays. *J Biomol Screen* **1999,** *4* (2), 67-73.

18. Kaplancıklıa,b, Z.A. Yurttaa,* L, Turan-Zitounia, G , Özdemira, A , Gögerc, G, Demircib,c, F. Mohsen, U. A., Synthesis and Antimicrobial Activity of New Pyrimidine-Hydrazones. *Letters, in Drug Design & Discovery*, **2014**, *11*, 76-81.

19. Altintop, M.D.; Kaplanciki, Z. A.; Ciftci, G. A.; Demirel, R., Synthesis and biological evaluation of thiazoline derivatives as newantimicrobial and anticancer agents. *European Journal of Medicinal Chemistry***, 2014***, 74,* 264-277

20. Lokwani, D.; Azad, R; Sarkate, A.; Reddanna, P.; Shinde, D. Structure Based Library Design (SBLD) for new 1,4-dihydropyrimidine scaffold as simultaneous COX-1/COX-2 and 5-LOX inhibitors, *Bioorganic & Medicinal Chemistry*, **2015**, *23 (15)*, 4533-4543.